

# Estimation of effective temperatures in a quantum annealer and its impact in sampling applications: A case study towards deep learning applications

Marcello Benedetti,<sup>1</sup> John Realpe-Gómez,<sup>1,2,3</sup> Rupak Biswas,<sup>4</sup> and Alejandro Perdomo-Ortiz<sup>1,5,\*</sup>

<sup>1</sup>Quantum Artificial Intelligence Lab., NASA Ames Research Center, Moffett Field, CA 94035, USA

<sup>2</sup>SGT Inc., 7701 Greenbelt Rd., Suite 400, Greenbelt, MD 20770, USA

<sup>3</sup>Instituto de Matemáticas Aplicadas, Universidad de Cartagena, Bolívar 130001, Colombia

<sup>4</sup>Exploration Technology Directorate, NASA Ames Research Center, Moffett Field, CA 94035

<sup>5</sup>University of California Santa Cruz @ NASA Ames Research Center, Moffett Field, CA 94035, USA

Sampling is at the core of deep learning and more general machine learning applications; an increase in its efficiency would have a significant impact across several domains. With the advent of more mature quantum computing technologies, quantum annealers have been proposed as a potential candidate to speed up these tasks, but several limitations still bar these state-of-the-art technologies from being used effectively. One of the main limitations, and the focus of this work, is that using the device's experimentally accessible temperature as a reference for sampling purposes leads to very poor correlation with the Boltzmann distribution it is programmed to sample from. Based on quantum dynamical arguments, one can expect that if the device indeed happens to be sampling from a Boltzmann-like distribution, it will correspond to one with an *instance-dependent* effective temperature. Unless this unknown temperature can be unveiled, it might not be possible to effectively use a quantum annealer for Boltzmann sampling processes. In this work, we propose a strategy to overcome this challenge with a simple effective-temperature estimation algorithm. To highlight the importance of this estimation, we provide a systematic study assessing the impact of the effective temperatures in the training of a kind of restricted Boltzmann machine on quantum hardware, which can serve as a building block for deep learning architectures. We also provide a comparison to  $k$ -step contrastive divergence(CD- $k$ ) with  $k$  up to 100 to have better assessment of the performance. Although our suggested quantum-assisted training algorithm as well as other simplifications that assume a fixed effective temperature clearly outperform conventional contrastive divergence (CD-1), only our algorithm is capable of matching CD-100 for the Boltzmann machine trained in this work.

## I. INTRODUCTION

The use of quantum computing technologies for sampling and machine learning applications is attracting increasing interest from the research community in recent years [1–15]. Although the main focus of the quantum annealing computational paradigm [16–18] has been in solving discrete optimization problems in a wide variety of application domains [19–26], it has been also introduced as a potential candidate to speed up computations in sampling applications. Indeed, it is an important open research question whether or not quantum annealers can sample from Boltzmann distributions more efficiently than traditional techniques [4, 5, 9].

However, there are some challenges that need to be overcome before uncovering the potential of quantum annealing hardware for sampling problems. One of the main difficulties is that the device does not necessarily sample from the Boltzmann distribution that would correspond to the physical temperature and the user-specified control parameters (couplings and fields) of the device. Instead, there might be some instance-dependent corrections leading, in principle, to instance-dependent effective temperature [4, 27, 28]. Bian *et al.* [4] has used the maximum likelihood method to estimate such an instance-dependent temperature and introduced some additional shifts in the control parameter of the quantum device, for several realizations of small eight-qubit instances on an early generation of quantum annealers produced by D-Wave Systems. The authors showed that, with these additional estimated shifts in place, the empirical probability distribution obtained from the D-Wave appears to correlate very well with the corresponding Boltzmann distribution. Further experimental evidence of this effective temperature can be found in Ref. [28] where a proper determination of this effective temperature was needed to determine residual bias in the programmable parameters of the device.

Recently some authors have explored the use of quantum annealing hardware for the training of Boltzmann machines and deep neural networks [4, 5, 9, 14]. Training a general Boltzmann machine or a deep neural

---

\*Electronic address: alejandro.perdomoortiz@nasa.gov

network is in general intractable due to long equilibration times of sampling techniques like Markov Chain Monte Carlo (MCMC). One of the strategies that have made possible the recent spectacular success [29] of these techniques is to deal with less general architectures that allow for substantial speedups. Restricted Boltzmann Machines (RBMs) [30, 31] are an important example of this kind that moreover serve as a suitable building block for deeper architectures. Still, quantum annealers has the potential to allow for training more complex architectures.

When applying quantum annealing hardware to the training of Boltzmann machines the interest is in finding the optimal control parameters that best represent the empirical distribution of a dataset. However, estimating additional shifts for the control parameters, as done by Bian *et al.* [4], would not be practical since it is in a sense similar to the very kind of problem that a Boltzmann machine attempts to solve. One could then ask what is the meaning of using a quantum annealer for learning the parameters of a distribution, if to do it we need to use standard techniques to learn the corrections to the control parameters.

Here we explore a different approach by taking into account only the possibility of an instance-dependent effective temperature without the need of considering further instance-dependent shifts in the control parameters. We devise a technique to estimate the effective temperature associated to a given instance by generating only two sets of samples from the machine and performing a linear regression. The samples used in our effective-temperature estimation algorithm are the same ones used towards achieving the final goal of the sampling application. This is in contrast with the approach taken in [4] which needs in principle many evaluations of the gradient of the log-likelihood of a set of samples from the device, making it impractical for large problem instances.

We test our ideas in the training of Boltzmann machines. In the next section we shall present a brief overview of the ideas related to Boltzmann machines and discuss how quantum annealing hardware can be used to assist their training. Afterwards we discuss related work. In the section that follows we introduce our technique to estimate the effective temperature associated to a given instance. We then show an implementation of these ideas for the quantum-assisted training (QuAT) of a Chimera-RBM on the Bars and Stripes dataset [32–34], implemented in the Dwave 2X device (DW2X) located at NASA Ames Research Center. Finally, we present the conclusions of the work and some perspectives of the future work we will be exploring.

## II. GENERAL CONSIDERATIONS

### A. General Boltzmann machines

Consider a data set  $\mathcal{D} = \{v^1, \dots, v^D\}$  whose empiric distribution is  $Q(v)$ ; here each datapoint can be represented as an array of Ising variables, i.e.  $v^d = (v_1^d, \dots, v_M^d)$  with  $v_i^d \in \{-1, +1\}$ . A Boltzmann machine models the data via a model distribution  $P(v) = \sum_u P_B(u, v)$ , where  $P_B(u, v) = e^{-E(u, v)}/Z$  is a Boltzmann distribution on a possibly extended sample space  $\{u, v\}$ ,  $E(u, v)$  is the corresponding energy function, and  $Z$  is the normalization constant or partition function. Notice that in this case we do not need a temperature parameter, since it only amounts at a rescaling of the *model parameters* that we want to learn. Here  $u = (u_1, \dots, u_N)$  are the ‘unseen’ or ‘hidden’ variables, that help capture higher level structure in the data, and  $v = (v_1, \dots, v_M)$  are the ‘visible’ variables, that correspond to the data themselves. Denoting these variables collectively by  $s = (u, v)$  we can write

$$E(s) = - \sum_{ij \in \mathcal{E}} W_{ij} s_i s_j - \sum_{i \in \mathcal{V}} b_i s_i, \quad (1)$$

where  $W_{ij}$  and  $b_i$  are the model parameters that has to be adjusted to fit the data; here  $\mathcal{V}$  and  $\mathcal{E}$  are the set of vertices and edges, respectively, that make up the interaction graph  $\mathcal{G} = (\mathcal{V}, \mathcal{E})$ .

The task is then to find the model parameters that make the model distribution  $P$  as close as possible to the data distribution  $Q$ . This can be accomplished by minimizing the KL divergence between  $Q$  and  $P$  or, equivalently, by maximizing the log-likelihood [34]

$$\mathcal{L} = \frac{1}{D} \sum_{d=1}^D \log P(v^d). \quad (2)$$

with respect to the model parameters  $W$  and  $b$ .

Gradient ascent is a standard method to carry out this optimization via the rule

$$W_{ij}^{(t+1)} = W_{ij}^{(t)} + \eta \frac{\partial \mathcal{L}}{\partial W_{ij}}, \quad (3)$$

$$b_i^{(t+1)} = b_i^{(t)} + \eta \frac{\partial \mathcal{L}}{\partial b_i}, \quad (4)$$

where  $\eta > 0$  is the learning rate, and the gradient of the log-likelihood function is given by [34]

$$\frac{\partial \mathcal{L}}{\partial W_{ij}} = [\langle s_i s_j \rangle_D - \langle s_i s_j \rangle_M], \quad (5)$$

$$\frac{\partial \mathcal{L}}{\partial b_i} = [\langle s_i \rangle_D - \langle s_i \rangle_M]. \quad (6)$$

Here  $\langle \cdot \rangle_D$  denotes the ensemble average with respect to the distribution  $P(u|v)Q(v)$  that involves the data. Similarly,  $\langle \cdot \rangle_M$  denotes the ensemble average with respect to the distribution  $P(u|v)P(v) = P_B(u, v)$  that involves exclusively the model. Such averages can be estimated by standard sampling techniques, such as MCMC. Another possibility, explored in this work, is to rely on a physical process that naturally generates samples from a Boltzmann distribution.

## B. Quantum annealing

Quantum annealing is an algorithm that attempts to exploit quantum effects to find the configurations with the lowest cost of a function describing a problem of interest [16–18]. It relies on finding a mapping of such a function into the energy function of an equivalent physical system. The latter is suitably modified to incorporate quantum fluctuations whose purpose is to maintain the system in its lowest-energy solution space.

In short, the algorithm consists in slowly transforming the ground state of an initial quantum system, that is relatively easy to prepare, into the ground state of a final Hamiltonian that encodes the problem to be solved. The device produced by D-Wave Systems [35, 36] is a realization of this idea for solving quadratic unconstrained optimization problems on binary variables. It implements the Hamiltonian

$$H(s) = A(s)H_D + B(s)H_P, \quad (7)$$

$$H_D = - \sum_{i \in \mathcal{V}_C} \sigma_i^x, \quad (8)$$

$$H_P = \sum_{ij \in \mathcal{E}_C} J_{ij} \sigma_i^z \sigma_j^z + \sum_{i \in \mathcal{V}_C} h_i \sigma_i^z, \quad (9)$$

where  $\sigma_i^{x,z}$  are Pauli matrices that operate on spin or qubit  $i$ . The *control parameters* of the D-Wave machine are composed of a field  $h_i$  for each qubit  $i$  and a coupling  $J_{ij}$  for each pair of interacting qubits  $i$  and  $j$ . The topology of the interactions between qubits in the D-Wave is given by a so-called Chimera graph  $\mathcal{C} = (\mathcal{V}_C, \mathcal{E}_C)$ . This is made up of elementary cells of  $4 \times 4$  complete bi-partite graphs that are coupled as shown in Fig. 1 (a). The transformation from the simple Hamiltonian  $H_D$  to the problem Hamiltonian  $H_P$  is controlled by time-dependent monotonic functions  $A(s)$  and  $B(s)$ , such that  $A(0) \gg B(0)$  and  $A(1) \ll B(1)$ . Here  $s = t/t_a$ , where  $t$  is the physical time and  $t_a$  is the annealing time, i.e. the time that it takes to transform Hamiltonian  $H_D$  into Hamiltonian  $H_P$ .

Although quantum annealers were designed with the purpose of reaching a ground state of the problem Hamiltonian  $H_P$ , there are theoretical arguments [27] and experimental evidence [4, 37] suggesting that under certain conditions the device samples from an approximately Boltzmann distribution at a given effective temperature. Such an effective temperature depends on the specific energy landscape that is realized, and so on the particular instance. How to exploit this sampling feature of the quantum device is the main focus of this work.

## C. Chimera Restricted Boltzmann machines

Training a general Boltzmann machine is in general intractable due to long equilibration time of sampling techniques like MCMC. One way to escape this issue is to use less general architectures. One of the most

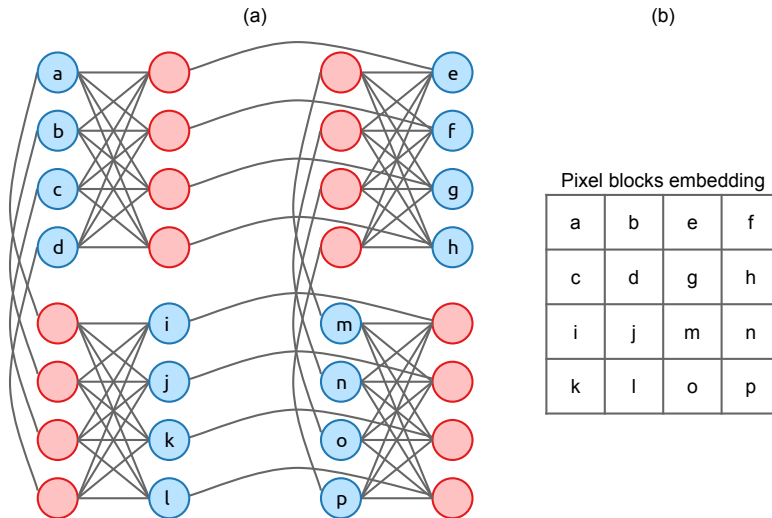


FIG. 1: *Chimera-RBM and data representation*: (a) D-Wave hardware embedding of a Chimera-RBM with 16 visible and 16 hidden variables. (b) Mapping of the pixels in the pictures to the visible units in the Chimera-RBM that has been used in this work (cf. [9]).

investigated architectures is the *Restricted Boltzmann Machine* (RBM). The interaction graph  $\mathcal{G}$  of an RBM is a fully bipartite graph in which visible and hidden units interact with each other but not among themselves. This implies that the conditional distributions  $P(v|u)$  and  $P(u|v)$  factorize in terms of single variable marginals, which substantially simplifies the problem of obtaining samples from them. This leads to the idea of  $k$ -step contrastive divergence learning (CD- $k$ ) where the model expectation values are approximated as follows: first we start with a datapoint  $v^{(0)}$ ; then we sample  $u^{(0)}$  from  $p(u|v^{(0)})$ , and subsequently sample  $v^{(1)}$  from  $p(v|u^{(0)})$  and so on for  $k$  steps. At the end of this process we obtain a sample  $v^{(k)}$  [34].

It is in principle possible to embed a restricted Boltzmann machine (RBM) in quantum annealing hardware [14]. However, due to limited connectivity of the device, the resulting physical representation would involve a larger number of physical variables (qubits) and of physical links (couplings) than the original RBM being represented. It would be preferable to use an alternative model that can be naturally represented in the device. For this reason we will focus on the kind of models that are obtained after removing from a given RBM all the links that are not present in the D-Wave machine [9]. We will call this type of models *Chimera Restricted Boltzmann Machines* (Chimera-RBM). Fig. 1 shows an example of a Chimera-RBM (a) and a possible embedding of the pixels of an image into its visible units (b).

### III. RELATED WORK

Dumoulin *et al.* [9] have studied the impact of different limitations of quantum annealing hardware for training restricted Boltzmann machines. The authors have focused on three kinds of limitations: noisy parameters, limited parameter range, and restricted architecture. The training method used was persistent contrastive divergence where the model ensemble averages were estimated with samples from simulated quantum hardware while the data ensemble averages were estimated by exact mean field.

For assessing the impact of limited connectivity, Dumoulin *et al.* investigated a Chimera-RBM. They found that limited connectivity is the most relevant limitation in this context. In a sense this is understandable as standard RBMs are based on complete bipartite graphs while the Chimera graph is sparse. Roughly speaking, this means that if the number of variables is of order  $N$ , the number of parameters present in a Chimera graph is a vanishing fraction (of order  $1/N$ ) of the number of parameters in the corresponding RBM. Furthermore, connections in the Chimera graph are rather localized. This feature may make more difficult to capture higher level correlations.

The authors also found that noisy parameters in an RBM is the next relevant limitation and that the noise in the couplings is more relevant than the noise in the fields. This could simply be due to the fact that the number of fields is a vanishing fraction (of order  $1/N$ ) of the number of couplings in an RBM. This argument is not valid anymore in a Chimera-RBM, though. Now, the authors also mention that the noise in the couplings is

‘quenched’, i.e. it only changes every time the coupling values change, while the noise in the fields is ‘annealed’, i.e. it changes in every sample generated. If this is indeed the case, this could be another reason for the higher relevance of the noise in the couplings than the noise in the fields.

Finally, an upper bound in the magnitude of the model parameters, similar to the one present in the D-Wave device, does not seem to have much impact. In this respect, we should notice that current D-Wave devices are designed with the aim of reaching only the ground state. In contrast, typical applications of Boltzmann machines deals with heterogeneous real data which contains a relatively large level of uncertainty, and are expected to exploit a wider range of configurations. This suggests that in sampling applications control parameters are typically smaller than those explored in applications to combinatorial optimization. This suggests that potential lower bounds in the magnitude of the control parameter can turn out to be more relevant for sampling applications. In this respect, it is important to notice that noise in the control parameters can lead to an effective lower bound.

While Dumoulin *et al.* modeled the instance-dependent corrections as independent Gaussian noise around the user defined parameter values, Denil and Freitas [5] devised a way to by-pass this problem altogether. For doing this, the authors have optimized the one-step reconstruction error as a black box function and approximate its gradient empirically. They do this by a technique called simultaneous perturbation stochastic approximation. However, with this approach it is not possible to decouple the model from the machine. Furthermore, it is not clear what is the efficiency of this technique nor how to extend it to deal with the more robust log-likelihood function rather than the reconstruction error. In their approach only the hidden layer is embedded in the D-Wave, and qubit interactions are exploited to build a semi-restricted Boltzmann machine. They report encouraging results, although they are still no conclusive since the log-likelihood function was not the function being optimized.

#### IV. QUANTUM-ASSISTED TRAINING OF BOLTZMANN MACHINES

A promising idea for training more general Boltzmann machines is to rely on a physical device, like D-Wave’s, that naturally generates samples from a Boltzmann distribution [4, 5, 9]. Due to various sources of noise, the D-Wave device produces samples from an approximately Boltzmann distribution, but at a temperature different from the physical temperature of the device. Indeed, there might be some instance-dependent corrections [4]; we will only take into account corrections to the temperature and neglect any possible shifts in the control parameters. We will assume a Boltzmann distribution defined by an energy function as in (1), with  $W_{ij} = J_{ij}/T_{\text{eff}}$  and  $b_i = h_i/T_{\text{eff}}$ , where  $T_{\text{eff}}$  can be instance-dependent. While the control parameters for the D-Wave are couplings and fields, i.e.  $J_{ij}$  and  $h_i$ , the learning takes place on the ratio of the control parameters to the temperature, i.e.  $W_{ij}$  and  $b_i$ . Inferring temperature is therefore a fundamental step in order to be able to use the samples from the D-Wave for learning. A learning algorithm for the quantum-assisted training (QuAT) of a Boltzmann machine needs access to a method that estimates the temperature at each iteration. The learning algorithm we propose is initialized as follows:

- Pick very small initial control parameters,  $J_{ij}^{(0)}$  and  $h_i^{(0)}$ , and generate two sets of samples from the device.
- Using the samples obtained in the previous item, estimate the corresponding temperature  $T_{\text{eff}}^{(0)}$  and compute the initial model parameters  $W_{ij}^{(0)} = J_{ij}^{(0)}/T_{\text{eff}}^{(0)}$  and  $b_i^{(0)} = h_i^{(0)}/T_{\text{eff}}^{(0)}$ .

Then it iterates as follows:

- Using the samples and model parameters obtained at step  $t$ , update the model parameters according to Eq. (3) to obtain  $W_{ij}^{(t+1)}$  and  $b_i^{(t+1)}$ .
- Obtain new control parameters by doing  $J_{ij}^{(t+1)} \approx T_{\text{eff}}^{(t)} W_{ij}^{(t+1)}$  and  $h_i^{(t+1)} \approx T_{\text{eff}}^{(t)} b_i^{(t+1)}$  and generate two sets of samples from the device.

A few comments are in order. First, the two sets of samples that we mention above are for estimating model and data ensemble averages. For the former we just need to run the device with the specified control parameters. For the latter we need to generate samples with the visible units clamped to the datapoints, which can be done by applying suitable fields to the corresponding qubits. However, in the case of restricted Boltzmann machines we can avoid this last step as it is possible to compute exactly the data ensemble averages. Second, notice that to compute the new control parameters at step  $t + 1$  we should have used temperature  $T_{\text{eff}}^{(t+1)}$  at

the same step. However, to obtain such a temperature we would need to know which are the parameters at time  $t + 1$ . To escape this vicious cycle we have done  $T_{\text{eff}}^{(t+1)} \approx T_{\text{eff}}^{(t)}$ . In the next section we discuss a method for estimating this instance-dependent temperature.

## V. TEMPERATURE ESTIMATION

Consider the Boltzmann distribution  $P(E; \beta) = g(E)e^{-\beta E}/Z(\beta)$  at a generic inverse temperature  $\beta$  as a function of the energy  $E$ . Here  $g(E)$  is the degeneracy of the energy level  $E$  and  $Z(\beta)$  is the partition function. We want to devise an efficient method for estimating the effective temperature associated to a given instance. To do this, consider the log-likelihood ratio of two different states or energy levels,  $E_1$  and  $E_2$ , given by

$$\ell(\beta) \equiv \log \frac{P(E_1; \beta)}{P(E_2; \beta)} = \log \frac{g(E_1)}{g(E_2)} - \beta \Delta E, \quad (10)$$

where  $\Delta E = E_1 - E_2$ . We can estimate this log-likelihood ratio by estimating the frequencies of the two states involved. We could in principle do this for different values of the parameter  $\beta$  by rescaling the control parameters of the device. Indeed, rescaling the control parameters by a factor  $x$  is equivalent to setting a parameter  $\beta = x\beta_{\text{eff}}$ , where  $\beta_{\text{eff}} = 1/T_{\text{eff}}$  is the inverse of the effective temperature  $T_{\text{eff}}$  associated to a given instance. Notice that this is only true under the assumption that  $T_{\text{eff}}$ , despite being instance-dependent, does not change appreciably under small rescalings of the control parameters. In this way, we can expect that by plotting the log-likelihood ratio  $\ell(x\beta_{\text{eff}})$  against the scaling parameter  $x$ , we should obtain a straight line whose slope and intercept are given by  $-\beta_{\text{eff}}\Delta E$  and  $\log[g(E_1)/g(E_2)]$ , respectively. Since we know the energy levels we can in principle infer  $\beta_{\text{eff}}$ . However, the performance of this method was rather poor in all experiments we did (not shown). A reason for this could be that to perform the linear regression to extract the corresponding effective temperature, several values of  $x$  need to be explored in a relatively wide range. Next we present a proposal that mitigate this limitation.

The previous approach relied on several values of the scaling parameter  $x$  but only two energy levels. We were not exploiting all the information available in the other states in the sample set from the quantum annealer. We can exploit such an information to obtain a more robust estimate of the temperature by sampling only for the original control parameters and a single rescaling of them. The idea here is to take the difference  $\Delta\ell \equiv \ell(\beta) - \ell(\beta')$  of the log-likelihood ratios of pairs of energy levels, with  $\beta = \beta_{\text{eff}}$  and  $\beta' = x\beta_{\text{eff}}$ , to eliminate the unknown degeneracies altogether, yielding

$$\Delta\ell = \log \frac{P(E_1; \beta)P(E_2; \beta')}{P(E_2; \beta)P(E_1; \beta')} = \Delta\beta\Delta E, \quad (11)$$

where  $\Delta\beta = \beta' - \beta = (x - 1)\beta_{\text{eff}}$ . In this way, by generating a second set of samples at a ‘suitable’ value of  $x$  and then taking the differences of, say, the most populated level and all the remaining relevant ones we can plot  $\Delta\ell$  Vs.  $\Delta E$ . According to Eq. (11) this is expected to be a straight line with slope given by  $(x - 1)\beta_{\text{eff}}$ . In this way we can in principle obtain  $\beta_{\text{eff}}$  by generating only a new set of samples for parameters scaled by  $x$ . The choice of  $x$  matters: if it is too small no informative changes, other than noise, would be detected; if it is too large some levels would become unpopulated and we would not be able to compare them at both the original and rescaled control parameters.

Fig. 2a shows an instance of temperature estimation using 1000 samples from the DW2X and a scaling parameter  $x = 0.6$ . Despite the dispersion of the data we can observe a somewhat robust behavior and a clear linear trend. A least squares linear regression of the data yields a temperature of  $T_{\text{eff}} = 0.091(4)$ . Fig. 2b shows a comparison of the performance of the temperature estimation technique for different values of the scaling parameter  $x$ , using  $x = 0.6$  as a reference. Overall we can see that  $x = 0.6$  typically displays a better performance. This value has also worked best for training a Chimera-RBM in the different experiments we have run. Notice also that although there is some dependency on the performance as a function of  $x$ , and  $x = 0.6$  seemed to be the best here, there is no strong dependence of this value so a rule of thumb of selecting  $x \in [0.6, 0.8]$  could be suggested.

## VI. TRAINING OF A BOLTZMANN MACHINE ASSISTED BY THE D-WAVE 2X

Now that we have at our disposal a robust temperature estimation technique, we can use it for training Boltzmann machines. We will focus here on the training of a Chimera-RBM. We decided to restrict to Chimera-RBM for two reasons. On the one hand, although an RBM can be embedded into quantum hardware [14], it

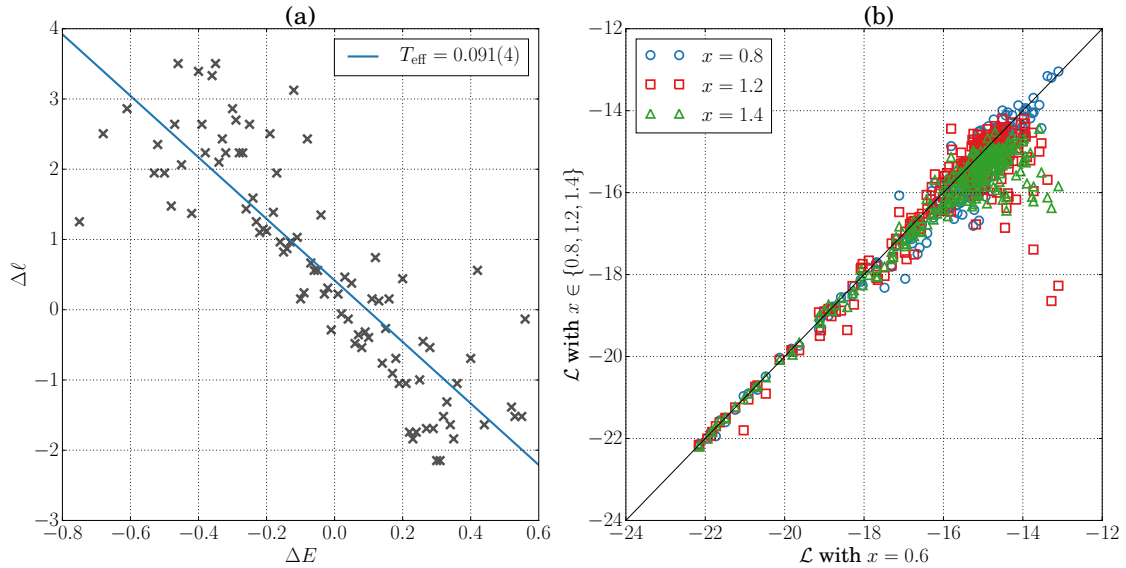


FIG. 2: *Temperature estimation:* (a) Log-likelihood ratio differences  $\Delta\ell$  in Eq. (11) estimated using 1000 samples for both the original and rescaled control parameters with  $x = 0.6$ . For doing this, we have first selected the most populated energy level at the original control parameters and have computed  $\Delta\ell$  corresponding to this energy level and all other energy levels that appear populated for both the original and rescaled control parameters. The straight line is obtained by a linear regression using least squares and predicts, according to Eq. (11), an effective temperature of  $T_{\text{eff}} = 0.091(4)$ . This was done for an arbitrary instance that appeared during the training of a Chimera-RBM on the BAS dataset (see Fig. 3). (b) Scatter plot of the log-likelihoods of the effective temperature estimated by using other values of  $x$  shown for comparison, using  $x = 0.6$  as a reference (horizontal axis).

requires to represent single variables with chains of qubits coupled via ferromagnetic interactions of a given strength. We consider that instead of forcing couplings to take a specific value in order to meet a preconceived design, it might be better to allow the learning algorithm itself to find the parameter values that work best for a particular application. On the other hand, the focus of our work is in better understanding the challenges that need to be overcome for using quantum annealers like DW2X for sampling applications, before moving forward to tackle problems of larger complexity.

To the best of our knowledge, this is the first systematic study providing both, an assessment of the use of the DWave in training Boltzmann machines and studying the impact of the effective temperature in the learning performance. We consider that it is important to assess the performance of the different training methods by exactly computing the log-likelihood during the training process. Otherwise, we could not be sure whether a difference in performance is due to the new training method or due to errors in the approximation of the log-likelihood. For this reason we tested the method in a small dataset called Bars and Stripes (BAS) and computed exhaustively the corresponding log-likelihood for evaluation. The BAS dataset consists of pictures generated by setting all the pixels of each row (or column) to either black (-1) or white (+1), at random [32–34]. A further technical difficulty that we meet is that while generating (say) 1000 samples in the DW2X for a given instance can take about 20 ms, the waiting time for accessing the machine to generate a new set of samples for a different instance can vary widely depending on the amount of jobs that are scheduled. So, while training a Chimera-RBM could take say about one hour had we exclusive access to the device, the waiting times of the different jobs can increase this time by an order of magnitude or so. Currently, we are running experiments with much larger instances and evaluating the performance in more tractable ways.

We modeled the BAS dataset with a Chimera-RBM of 16 visible and 16 hidden units with the topology shown in Fig. 1 (a). The mapping of pixels to visible units is shown in Fig. 1 (b) (cf. [9]). Fig. 3 (a) shows the evolution of the log-likelihood during the training of a Chimera-RBM on the BAS dataset under different learning algorithms, all of them with learning rate  $\eta = 0.1$ . We can observe that the quantum assisted training algorithm with effective-temperature estimation at each iteration (QuAT@ $T_{\text{eff}}$ , blue diagonal crosses  $\times$ ) outperforms CD-1 (blue solid squares) after about 300 iterations. However, within the 3000 iterations shown in the figure, QuAT@ $T_{\text{eff}}$  has not yet been able to outperform CD-25 nor CD-100, although there is a clear trend in that direction. Interestingly, CD- $k$  reaches their best log-likelihood values after a relatively small number of iterations while QuAT@ $T_{\text{eff}}$ , in contrast, increases slowly and steadily. One may be inclined

to think this is because CD- $k$  estimates the model averages from samples that are generated by running a  $k$ -step Markov chain initialized at each data point. In this way CD- $k$  is using information contained in the data from the very beginning for the estimation of the model ensemble averages, while QuAT@ $T_{\text{eff}}$  ignores them altogether. However, if this were indeed the case one should expect such a trend to diminish for increasing values of  $k$ , something that is not observed in the figure. A better understanding of this point has the potential to considerably improve the performance of QuAT@ $T_{\text{eff}}$ .

To assess the relevance of temperature estimation for QuAT@ $T_{\text{eff}}$ , we also show in Fig. 3 the evolution of the log-likelihood under quantum assisted training at a fixed temperature  $T = T_0$  (QuAT@ $T = T_0$ ). First, we can observe that using the physical temperature of the device (pink empty squares in Fig. 3 (b)), which is estimated to be  $T_{\text{DW2X}} = 0.033$  (12.5 mK), leads to a very poor performance. Fixing the temperature to the average  $T_{\text{av}} = 0.118$  over all temperatures found during the run of QuAT@ $T_{\text{eff}}$  discussed before leads to a better performance (red empty circles) but still well below that displayed by QuAT@ $T_{\text{eff}}$  itself. Interestingly, fixing the temperature to  $T_{\text{eff}} = 0.08 < T_{\text{av}}$  leads to a better performance than that displayed with  $T_{\text{av}}$ , still below the performance of QuAT@ $T_{\text{eff}}$ . Fixing the effective temperature to  $T_{\text{eff}} = 0.16 > T_{\text{av}}$ , on the other hand, leads to a decrease in performance with respect to that displayed with  $T_{\text{av}}$ .

Fig. 3 (c) shows the effective temperatures estimated at each iteration of QuAT@ $T_{\text{eff}}$  of the Chimera-RBM on the BAS dataset. We can observe that it starts with values closed to the temperature of the device  $T_{\text{DW2X}}$  and starts increasing, initially at a steady pace and then with a slower trend.

## VII. CONCLUSIONS AND FUTURE WORK

Training a general Boltzmann machine is in general intractable due to long equilibration times of sampling techniques like MCMC. In this work we propose a strategy to overcome one of the main limitations when intending to use a quantum annealer to sample from Boltzmann distributions: the determination of effective temperatures in quantum annealers. The simple technique proposed in this work uses the samples obtained from the quantum annealer (the DW2X at NASA is our experimental implementation) to estimate both, the effective temperature and the hard-to-compute term in the log-likelihood gradient, i.e., the averages over the model distribution, needed to determine the next step in the training process. We present a systematic study of the impact of the effective-temperature in the training of a Chimera-RBM model with 16 visible and 16 hidden units, and we compare the different settings with different effective temperatures to the performance of a CD- $k$  implementation, with  $k$  up to 100.

The Chimera-RBM model itself is much less powerful than the full RBM model. While the former is sparse with a number of parameters increasing linearly with the number of variables, the latter is dense with a number of parameters increasing quadratically instead. RBMs have the nice feature that sampling in one layer (conditioned to a configuration in the other layer) can be done in parallel and in one step; this is one of the key features of full RBMs and the main reason for their wide adoption. This nice feature does not hold true anymore once we have non-trivial lateral connections in one of the layers, which is the concept behind more powerful general BMs, and where we think it is one for the most promising direction to explore with the quantum-assisted training (QuAT) algorithms. By restricting QuAT to study Chimera-RBM models (or, in general, RBM models), one is paying the price of using a device that is in principle more powerful, but we are not taking the gains of having a more general model. It is important to investigate how to take full advantage of the DW2X by designing more suitable models based on the Chimera graph. An interesting possibility is the one explored in Ref. [9] where the Chimera graph of the DW2X is used as a hidden layer to build a semi-restricted Boltzmann machine, which therefore have lateral connections in the hidden layer.

However, the goal of this first QuAT implementation on small Chimera-RBMs serves several purposes. When dealing with large datasets the log-likelihood cannot be exhaustively computed due to the intractability of computing the partition function. Log-likelihood is the gold standard metric but it becomes intractable for large systems. In these cases, other performance metrics have been used such as reconstruction error or cross entropy error, and although widely used these are not 100% reliable for our benchmarking purpose [38]. Since these other proxies are meant to approximate the log-likelihood, if we were to use these we could not be sure that we would be drawing the right conclusions. This justifies why we used a moderately small dataset with 16 visible and 16 hidden units, and even though computing the log-likelihood was computational intensive for the study performed here, having 32 units in total was still a manageable size. Through the computation of the exact likelihood we were able to examine in more detail some of the goals proposed here: being able to assess the best effective temperature fit to the desired Boltzmann distribution and to show that using a constant temperature different from the estimated one with our approach might lead to severe suboptimal setting in terms of the training performance.



FIG. 3: *Comparison of learning algorithms for a Chimera-RBM:* (a) Evolution of the log-likelihood during the training process of a Chimera-RBM on the BAS dataset. The log-likelihood has been evaluated exhaustively every 50 iterations. The (blue) diagonal crosses ( $\times$ ) correspond to quantum-assisted training estimating effective temperatures (QuAT@ $T_{\text{eff}}$ ) with the DW 2X using 1000 samples in each iteration for the estimation of both temperature (twice,  $x = 0.6$  and  $x = 1.0$ ) and log-likelihood gradient. The (red) empty circles correspond to fixed-temperature quantum-assisted training algorithm (QuAT@ $T_{\text{av}} = 0.1177$ ), using the average temperature  $T_{\text{av}}$  found during the run of QuAT@ $T_{\text{eff}}$ . The vertical lines ( $|$ ) and empty triangles correspond to fixed-temperature quantum-assisted training algorithm (QuAT@ $T = T_0$ ) using temperatures above ( $T_0 = 0.16$ ) and below ( $T_0 = 0.08$ ) the average temperature  $T_{\text{av}}$ , respectively. The filled squares, circles, and triangles correspond to training using CD- $k$  for  $k = 1, 25, 100$ , respectively. (b) The (pink) empty squares correspond to the fixed-temperature quantum-assisted training algorithm (QuAT@ $T_{\text{DW}2\text{X}} = 0.033$ ), using the physical temperature of the device  $T_{\text{DW}2\text{X}} = 0.033$  (12.5 mK); notice that, even though the initial conditions are the same, it immediately drops to very negative values. (c) Temperatures estimated at each iteration during the run of the QuAT@ $T_{\text{eff}}$  with  $x = 0.6$ . (See Appendix A for a more systematic study.)

Another aspect we explore in this study was to go beyond the conventional CD-1, with the purpose of having a more fair comparison to the results that might be expected from the entirely classical algorithm counterpart. Previous results from our research group [39], as well as others reported by other researchers [14, 40], are limited to comparing the performance of quantum annealers to the quick but suboptimal CD-1. As shown in those studies, even with a suboptimal constant temperature one might be drawn to conclude that QuAT is outperforming conventional CD. Similar conclusions might be drawn from the curves for constant but suboptimal  $T = 0.08$  and  $T_{\text{av}} = 0.1177$  vs. CD-1 in Fig. 3. As shown in Fig. 3, this conclusion does not hold anymore for higher values of  $k$ , while the method using the effective-temperature estimation proposed here is the only one showing a steady increase in performance, close to matching the largest value of  $k$  tried here, i.e.  $k = 100$ . A follow up study of this work will assess how close QuAT is following the exact log-likelihood gradient during the training and how different are the distributions learned with the classical algorithm and

the ones obtained with the QuAT algorithm.

Another important point that we are currently studying is whether the differences observed in performance remain for larger and more complex datasets. We would expect that the performance of CD- $k$  degrades with larger number of variables as equilibration times are expected to grow fast with the number of variables once the probability distribution starts having non-trivial structure. From this perspective, it is important to notice that QuAT is expected to display a more uniform exploration of configuration space. This feature may render unnecessary adding auxiliary terms to prevent distortions in the learning process. Indeed, CD- $k$  is usually regularized by adding a term that penalizes the size of the weights and that, if properly tuned, can avoid the drop in likelihood [34]. We can observe this effect in Fig. 3 after about 500 iterations for CD-1 and about 800 iterations for CD-25, for instance. QuAT, instead, increases the likelihood slowly but steadily without the need of an explicit regularization, at least within the 3000 iterations that we have investigated.

Several other interesting studies follow from having a robust method for estimating  $T_{\text{eff}}$ , and that we will be exploring to speedup the first version of our first QuAT protocol proposed here. For example, it seems reasonable to estimate it only in every certain number of training iterations. From Fig. 3 it can be seen that a good strategy would be to do it more frequently at the beginning and less frequent as it stabilizes or seem to converge around certain value. Still this has the drawback that if by any chance the temperature happens to be estimated badly, such an error would persist for several iterations. Another simple strategy not used in this study is to recycle also the samples taken at the value of  $x \neq 1$  and that was used thus far only for the estimation of  $T_{\text{eff}}$ . Since the two distributions are expected to be close enough, importance sampling as used in Ref. [4] can be used to connect the obtained samples and still use them in the model average computed along with the samples at  $x = 1$ .

There are other ways in which the ideas explored here could be extended. For instance, we can go beyond restricted Boltzmann machines to build deep learning architectures or beyond unsupervised learning to build discriminative models. In principle the speed of learning could be increased by adding a ‘momentum’ term to the gradient-ascent learning rule [34]. Indeed, Addachi and Henderson have started exploring these ideas in a contemporary work [14]. Instead, we have focused on first trying to better understand the basics before adding more (classical) complexity to the learning algorithms that we feel have the risk that it might obscure the actual contributions from the new approach.

Note that since CD- $k$  seems to be faster than the QuAT in the first iterations in Fig. 3, having the capabilities of efficiently estimating effective temperatures allows us for a simple hybrid classical-quantum learning approach. For example, one can think of using the classical algorithm to be used to generate a reasonably good starting Boltzmann model for the QuAT algorithm. More specifically, one could use the simple and cheap CD-1 until the learning progress plateaus, and then use the expensive QuAT to bootstrap and enhance the classically obtained model. This may be useful in helping to diminish the larger impact that the noise in the device might have when the control parameters are somewhat small. This work will be explored in detail in a following publication.

### Acknowledgements

This work was supported by NASA Ames Research Center. The authors would like to thank V. M. Janakiraman, Z. Jiang, T. Lanting, E. Rieffel, and N. Wiebe for useful discussions.

### Appendix A: Supplementary information

See Fig. 4 and Fig. 5.

- 
- [1] H. Neven, V. S. Denchev, G. Rose, and W. G. Macready, “Training a binary classifier with the quantum adiabatic algorithm,” *arXiv:0811.0416*, 2008.
  - [2] H. Neven, V. S. Denchev, M. Drew-Brook, J. Zhang, W. G. Macready, and G. Rose, “NIPS 2009 demonstration: binary classification using hardware implementation of quantum annealing,” 2009.
  - [3] H. Neven, V. S. Denchev, G. Rose, and W. G. Macready, “Training a large scale classifier with the quantum adiabatic algorithm,” *arXiv:0912.0779*, 2009.
  - [4] Z. Bian, F. Chudak, W. G. Macready, and G. Rose, “The Ising model: teaching an old problem new tricks,” 2010.

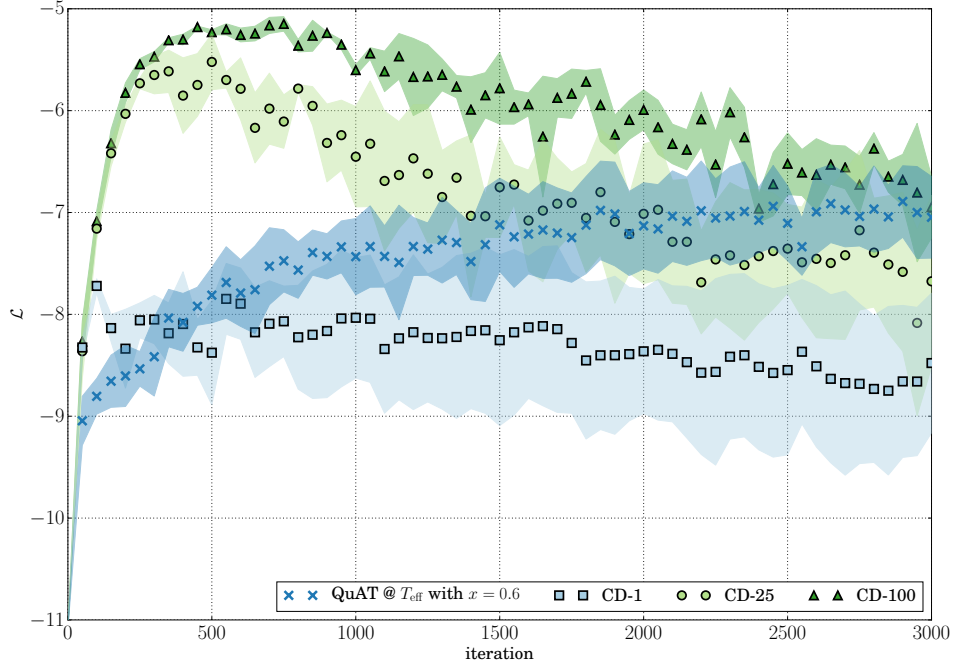


FIG. 4: Comparison of  $\text{QuAT}@T_{\text{eff}}$  with  $\text{CD}-k$  using three different runs in the same cell of the D-Wave chip. See Fig. 3 for details.

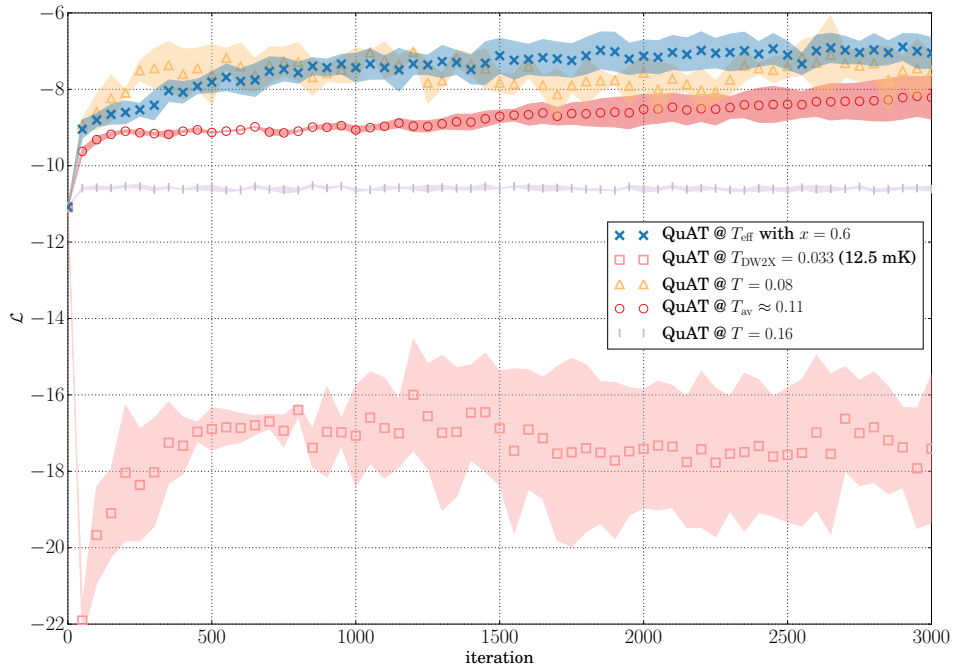


FIG. 5: Comparison of  $\text{QuAT}@T_{\text{eff}}$  with  $\text{QuAT}@T = T_0$  with different constant temperatures, using three different runs in the same cell of the D-Wave chip. See Fig. 3 for details.

- [5] M. Denil and N. De Freitas, “Toward the implementation of a quantum RBM,” *NIPS Deep Learning and Unsupervised Feature Learning Workshop*, 2011.
- [6] V. S. Denchev, N. Ding, S. Vishwanathan, and H. Neven, “Robust classification with adiabatic quantum optimization,” *arXiv:1205.1148*, 2012.
- [7] S. Lloyd, M. Mohseni, and P. Rebentrost, “Quantum algorithms for supervised and unsupervised machine learning,” *arXiv:1307.0411*, 2013.

- [8] K. Pudenz and D. Lidar, “Quantum adiabatic machine learning,” *Quantum Information Processing*, vol. 12, no. 5, pp. 2027–2070, 2013.
- [9] V. Dumoulin, I. J. Goodfellow, A. C. Courville, and Y. Bengio, “On the challenges of physical implementations of RBMs,” in *Proceedings of the Twenty-Eighth AAAI Conference on Artificial Intelligence, July 27 -31, 2014, Québec City, Québec, Canada.*, pp. 1199–1205, 2014.
- [10] S. Lloyd, M. Mohseni, and P. Rebentrost, “Quantum principal component analysis,” *Nat Phys*, 2014.
- [11] P. Rebentrost, M. Mohseni, and S. Lloyd, “Quantum support vector machine for big data classification,” *Phys. Rev. Lett.*, vol. 113, p. 130503, Sep 2014.
- [12] K. M. S. Nathan Wiebe, Ashish Kapoor, “Quantum deep learning,” *arXiv:1412.3489*, 2015.
- [13] S. Aaronson, “Read the fine print,” *Nat Phys*, vol. 11, pp. 291–293, Apr 2015. Commentary.
- [14] M. P. H. Steven H. Adachi, “Application of quantum annealing to training of deep neural networks,” *arXiv:1510.06356*, 2015.
- [15] N. Chancellor, S. Szoke, W. Vinci, G. Aeppli, and P. A. Warburton, “Maximum-entropy inference with a programmable annealer,” *arXiv:1506.08140*, 2015.
- [16] A. Finnila, M. Gomez, C. Sebenik, C. Stenson, and J. Doll, “Quantum annealing: a new method for minimizing multidimensional functions,” *Chemical physics letters*, vol. 219, no. 5, pp. 343–348, 1994.
- [17] T. Kadowaki and H. Nishimori, “Quantum annealing in the transverse ising model,” *Phys. Rev. E.*, vol. 58, p. 5355, Nov. 1998.
- [18] E. Farhi, J. Goldstone, S. Gutmann, J. Lapan, A. Lundgren, and D. Preda, “A quantum adiabatic evolution algorithm applied to random instances of an NP-Complete problem,” *Science*, vol. 292, pp. 472–475, Apr. 2001.
- [19] F. Gaitan and L. Clark, “Ramsey numbers and adiabatic quantum computing,” *Phys. Rev. Lett.*, vol. 108, p. 010501, Jan 2012.
- [20] A. Perdomo-Ortiz, N. Dickson, M. Drew-Brook, G. Rose, and A. Aspuru-Guzik, “Finding low-energy conformations of lattice protein models by quantum annealing,” *Sci. Rep.*, vol. 2, p. 571, Aug 2012.
- [21] Z. Bian, F. Chudak, R. Israel, B. Lackey, W. G. Macready, and A. Roy, “Discrete optimization using quantum annealing on sparse ising models,” *Frontiers in Physics*, vol. 2, no. 56, 2014.
- [22] B. O’Gorman, R. Babbush, A. Perdomo-Ortiz, A. Aspuru-Guzik, and V. Smelyanskiy, “Bayesian network structure learning using quantum annealing,” *The European Physical Journal Special Topics*, vol. 224, no. 1, pp. 163–188, 2015.
- [23] E. G. Rieffel, D. Venturelli, B. O’Gorman, M. B. Do, E. M. Prystay, and V. N. Smelyanskiy, “A case study in programming a quantum annealer for hard operational planning problems,” *Quantum Information Processing*, vol. 14, no. 1, pp. 1–36, 2015.
- [24] Perdomo-Ortiz, A., Fluegemann, J., Narasimhan, S., Biswas, R., and Smelyanskiy, V.N., “A quantum annealing approach for fault detection and diagnosis of graph-based systems,” *Eur. Phys. J. Special Topics*, vol. 224, no. 1, pp. 131–148, 2015.
- [25] A. Perdomo-Ortiz, J. Fluegemann, R. Biswas, and V. N. Smelyanskiy, “A performance estimator for quantum annealers: gauge selection and parameter setting,” *arXiv:1503.01083*, 2015.
- [26] D. Venturelli, D. J. Marchand, and G. Rojo, “Quantum annealing implementation of job-shop scheduling,” *arXiv:1506.08479*, 2015.
- [27] M. Amin, “Searching for quantum speedup in quasistatic quantum annealers,” *arXiv:1503.04216*, 2015.
- [28] A. Perdomo-Ortiz, B. O’Gorman, J. Fluegemann, R. Biswas, and V. N. Smelyanskiy, “Determination and correction of persistent biases in quantum annealers,” *arXiv:1503.05679*, 2015.
- [29] Y. LeCun, Y. Bengio, and G. Hinton, “Deep learning,” *Nature*, vol. 521, pp. 436 – 444, 2015.
- [30] P. Smolensky, “Parallel distributed processing: Explorations in the microstructure of cognition, vol. 1,” ch. Information Processing in Dynamical Systems: Foundations of Harmony Theory, pp. 194–281, Cambridge, MA, USA: MIT Press, 1986.
- [31] G. E. Hinton, “Training products of experts by minimizing contrastive divergence,” *Neural computation*, vol. 14, no. 8, pp. 1771–1800, 2002.
- [32] G. E. Hinton and T. J. Sejnowski, “Parallel distributed processing: Explorations in the microstructure of cognition, vol. 1,” ch. Learning and Relearning in Boltzmann Machines, pp. 282–317, Cambridge, MA, USA: MIT Press, 1986.
- [33] D. J. C. MacKay, *Information Theory, Inference & Learning Algorithms*. New York, NY, USA: Cambridge University Press, 2002.
- [34] A. Fischer and C. Igel, “An introduction to restricted Boltzmann machines,” in *Progress in Pattern Recognition, Image Analysis, Computer Vision, and Applications*, pp. 14–36, Springer, 2012.
- [35] M. W. Johnson, M. H. S. Amin, S. Gildert, T. Lanting, F. Hamze, N. Dickson, R. Harris, A. J. Berkley, J. Johansson, P. Bunyk, E. M. Chapple, C. Enderud, J. P. Hilton, K. Karimi, E. Ladizinsky, N. Ladizinsky, T. Oh, I. Perminov, C. Rich, M. C. Thom, E. Tolkacheva, C. J. S. Truncik, S. Uchaikin, J. Wang, B. Wilson, and G. Rose, “Quantum annealing with manufactured spins,” *Nature*, vol. 473, pp. 194–198, May 2011.
- [36] R. Harris, M. W. Johnson, T. Lanting, A. J. Berkley, J. Johansson, P. Bunyk, E. Tolkacheva, E. Ladizinsky, N. Ladizinsky, T. Oh, F. Cioata, I. Perminov, P. Spear, C. Enderud, C. Rich, S. Uchaikin, M. C. Thom, E. M. Chapple, J. Wang, B. Wilson, M. H. S. Amin, N. Dickson, K. Karimi, B. Macready, C. J. S. Truncik, and G. Rose, “Experimental investigation of an eight-qubit unit cell in a superconducting optimization processor,” *Phys. Rev. B*, vol. 82, p. 024511, Jul 2010.
- [37] A. Perdomo-Ortiz, B. O’Gorman, J. Fluegemann, R. Biswas, and V. N. Smelyanskiy, “Determination and correction

- of persistent biases in quantum annealers,” *arXiv:1503.05679*, 2015.
- [38] G. E. Hinton, “A practical guide to training restricted boltzmann machines.,” in *Neural Networks: Tricks of the Trade (2nd ed.)* (G. Montavon, G. B. Orr, and K.-R. Müller, eds.), vol. 7700 of *Lecture Notes in Computer Science*, pp. 599–619, Springer, 2012.
- [39] M. Benedetti, “Exploring Quantum Annealing for Data Mining,” Master’s thesis, Université Lumière Lyon 2, France, 2015.
- [40] G. Rose, “First ever DBM trained using a quantum computer.” <https://dwave.wordpress.com/2014/01/06/first-ever-dbm-trained-using-a-quantum-computer/>, 2014. [Online; accessed 22-October-2015].